EVALUATION OF DIGITAL SPECKLE FILTERS FOR ULTRASOUND IMAGES

by

FARA NABILA BINTI RADZI

13796

Dissertation submitted to the Department of Electrical & Electronic Engineering in

Partial Fulfilment of the requirements for the

Degree Bachelor of Engineering (Hons)

(Electrical and Electronic Engineering)

Universiti Teknologi PETRONAS

Bandar Sri Iskandar

31750 Tronoh

Perak Darul Ridzuan

CERTIFICATION OF APPROVAL

EVALUATION OF DIGITAL SPECKLE FILTERS FOR ULTRASOUND IMAGES

by

FARA NABILA BINTI RADZI

13796

A project dissertation submitted to the

Department of Electrical and Electronic Engineering

Universiti Teknologi PETRONAS

in partial fulfilment of the requirement for the

Bachelor of Engineering (Hons)

(Electrical and Electronic Engineering)

Approved by,

_____

(Ms. Norashikin Yahya)

Project Supervisor

UNIVERSITI TEKNOLOGI PETRONAS

TRONOH, PERAK

September 2014

CERTIFICATION OF ORIGINALITY

This is to certify that I am responsible for the work submitted in this project, that the original work is my own except as specified in the references and acknowledgements, and that the original work contained herein have not been undertaken or done by unspecified sources or persons.

_____

(FARA NABILA BINTI RADZI)

ABSTRACT

Ultrasound (US) images are inherently corrupted by speckle noise causing inaccuracy of medical diagnosis using this technique. Hence, numerous despeckling filters are used to denoise US images. However most of the despeckling techniques cause blurring to the US images. In this work, four filters namely Lee, Wavelet Linear Minimum Mean Square Error (LMMSE), Speckle-reduction Anisotropic Diffusion (SRAD) and Non-local-means (NLM) filters are evaluated in terms of their ability in noise removal and capability to preserve the image contrast. This is done through calculating four performance metrics Peak Signal to Noise Ratio (PSNR), Ultrasound Despeckling Assessment Index (USDSAI), Normalized Variance and Mean Preservation. The experiments were conducted on three different types of images which is simulated noise images, computer generated image and real US images. The evaluation in terms of PSNR, USDSAI, Normalized Variance and Mean Preservation shows that NLM filter is the best filter in all scenarios considering both speckle noise suppression and image restoration however with quite slow processing time. It may not be the best option of filter if speed is the priority during the image processing. Wavelet LMMSE filter is the next best performing filter after NLM filter with faster speed.

ACKNOWLEDGEMENT

First and foremost, all praises to Allah S.W.T. for without His blessings I will not be able to complete this Final Year Project.

I would like to take this golden opportunity to express my sincere gratitude to my dedicated supervisor, Ms. Norashikin Yahya, for her sincere guidance, advice and support throughout the whole period of my Final Year Project. Throughout the course she has constantly provided precious knowledge and passionate motivations. The success of this project will indeed be impossible without her involvements and contributions. Besides, I would also like to thank Department of Electrical and Electronic Engineering, Universiti Teknologi PETRONAS for creating the opportunity that allows me to execute this project.

Last but not least, millions of thanks to my beloved family who has continuously supported and motivated me to work towards the completion of my Final Year Project.

TABLE OF CONTENTS

LIST OF TABLES

LIST OF GRAPHS

LIST OF FIGURES

LIST OF ABBREVIATIONS

US	**Ultrasound**
SRAD	**Speckle Reduction Anisotropic Diffusion**
NLM	**Non-local-means**
LMMSE	**Linear Minimum Mean Square Error**
FFT	**Fast Fourier Transform**
PDE	**Partial Differential Equation**
ICOV	**Instantaneous Coefficient Variation**
PSNR	**Peak Signal to Noise Ratio**
USDSAI	**Ultrasound Despeckling Assessment Index**

CHAPTER 1

INTRODUCTION

1.1 Background Study

Application of ultrasound (US) in medicine began as early as during the Second World War and has been developing rapidly ever since [1]. Ultrasound imaging is a very essential technique in medical diagnosis due to its safe, economical and non-invasive nature. Technically ultrasound images are formed from the echo signals that are reflected back to the transducers from the tissues or organs [2].

These echoes are formed through two processes, namely scattering and specular reflection. Scattering takes place when sound waves encounter entities which are smaller or similar to the wavelength of the pulse signal. On the other hand specular reflection takes place when larger (than the wavelength) entities are encountered. Scattering gives rise to overlapping echoes that undergo a phenomenon called interference which results in speckle being formed [3].

Therefore it can be said that US images are inherently corrupted with speckle, a form of noise which attenuates US images qualities, causing image interpretation and processing a tough task. Speckle can be characterized as irregular coarse patterns of spots. They reduce US image contrast causing difficulties in deriving useful information for both non-specialists and experts. Hence, there are many efforts made by researches to formulate various despeckling methods for denoising US images.

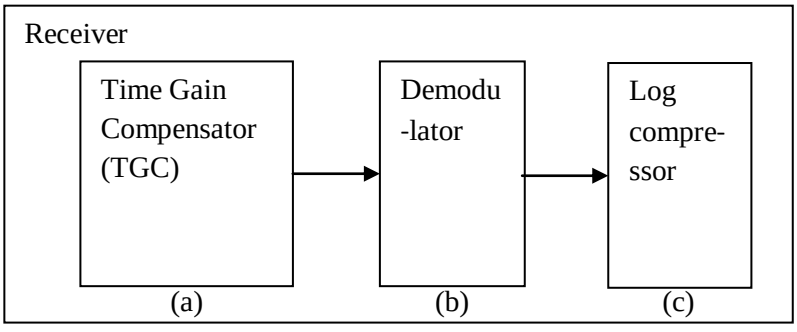

Figure 1: Receiver of ultrasound scanner (modified from [1])

In order for despeckling filters to be developed, it is crucial to accurately formulate statistical noise model. According to [2], the returned echoes are discovered to be having histogram of amplitudes that follows Rayleigh probability distribution function

$$\gamma_R(u) = \frac{u}{r^2}\exp\left(-\frac{\mathrm{u}^2}{2\mathrm{r}^2}\right), u \geq 0, \quad (1)$$

where u is real number and r is raw moments of Rayleigh distribution. Throughout this study the Rayleigh model will be utilized. The actual output of the demodulator in the receiver of ultrasound scanner shown in Fig. 1(b) can be expressed as

$$z(i,j) = x(i,j).n(i,j) + g(i,j), \quad (2)$$

where $z(i,j)$ represents the pixel corrupted with speckle, $x(i,j)$ represents noise-free pixel, $n(i,j)$ and $g(i,j)$ represents multiplicative and additive noise respectively. Meanwhile, i and j represent the rows and columns in 2-D image. However, since the effect of additive noise is significantly smaller than multiplicative noise and can be assumed negligible, the equation (2) can be re-written as

$$z(i,j) \approx x(i,j).n(i,j), \quad (3)$$

which makes speckle noise modeled as purely multiplicative. After log compression by log compressor as depicted in Figure 1(b) the speckle adopts the form of

$$\log(z(i,j)) = \log(x(i,j)) + \log(n(i,j)), \quad (4)$$

and can be simplified into

$$z_l(i,j) = x_l(i,j) + n_l(i,j). \quad (5)$$

There are various filters that have been derived by the researches that aim to remove the speckle and at the same time enhance the contrast while preserving the edges of the US images. These filters can be categorized according to their types such as linear, diffusion, non-local means and wavelet. Some of the common filters are Lee, Kuan, Frost, Wiener, AD, wavelet (LMMSE), SRAD and NLM. The summarization of several common despeckling filters is shown in the Table 1.

Despite the effective ability of the filters to remove the speckle there are also adverse effects from filtering, such as blurring of the details and edges as well as loss of information, since some speckle contain texture information [4]. In this study a few filters are selected from a few different categories (linear, diffusion, wavelet and non-local-means) to be analyzed and applied as the US image despeckling method. They are Lee, Speckle-reduction anisotropic diffusion (SRAD), NLM and wavelet (LMMSE) filters. The performance will not be evaluated solely in terms of speckle removal but also in contrast preservation capability.

Table 1: Summary of common despeckling filters

Types	Brief descriptions of methods	Investigators	Names
Linear	Utilize ratio of local statistics	[5]	Lee
	Based on minimum-mean-square error	[6]	Kuan
	Exponential model averaging filter	[7]	Frost
Non-linear	Utilized fast fourier transform (FFT) and inverse FFT	[8]	Homomorphic
Diffusion	Used partial differential equation (PDE)	[9]	anisotropic diffusion (AD)
	Utilized instantaneous coefficient variation (ICOV)	[10]	SRAD
Wavelet	Computed wavelet transform and wavelet coefficients are used	[11]	LMMSE
Non-local-means	Based on the self-similarity concept	[12]	Non-local-means (NLM)

More detailed concepts of the Lee, SRAD, wavelet (LMMSE) and NLM filters that will be used for this comparative study are disclosed in chapter 2 of section 2.1.

1.2 Problem statement

It is impossible for US images to be noise-free as naturally there will always be speckle noise due to backscattered echo. Therefore there are numerous speckle filters designed by researchers in effort to denoise medical US images. However most of these filters will cause blurring effect and are unable to maintain the originality of the US images. Majority of the studies in this field perform evaluation on the basis of speckle removal only but not on other aspects such as the filters' ability to retain textures, contrast and edges. This study provides an evaluation study of the filters' ability in noise removal and image restoration through various assessment metrics.

1.3 Objectives and Scopes of Study

1. Objectives

The main objective of this project is to produce an evaluation study of various speckle filters namely Lee, SRAD, NLM and wavelet (LMMSE) through various performance metrics PSNR, USDSAI, Normalized Variance and Mean Preservation.

2. Scopes of Study

The scope of this project also includes:

- Study and analysis of speckle noise model
- Study and analysis of performance evaluation metrics
- Study and analysis of the selected filters

CHAPTER 2

LITERATURE REVIEW

2.1 Despeckle Filters

This section discusses the theories of each filter that will be used in this paper. The filters are Lee, SRAD, Zhang LMMSE and NLM.

2.1.1 Lee Filter

Lee filter utilizes local statistics to perform edge preservation [5]. This filter also adopts the approach of using variance as a point of assessment whether smoothing is to be conducted or not. Edges are assumed to have high variance and therefore areas with high variance will not be smoothed meanwhile areas with less variance will be smoothed [13]. Lee filter can be expressed as

$$W(X,Y) = 1 - \frac{C_B^2}{C_I^2 + C_B^2} \tag{6}$$

where $W(X,Y)$ is the adaptive filter coefficient, C_I is the coefficient of variation of noisy image and C_B is the coefficient of variation of noise. Since Lee filter is based on first order statistical model, its performance is greatly affected by the window size and shape [13].

2.1.2 SRAD Filter

As mentioned by [14] this method is capable of removing speckle without eliminating image information and also preserve edges. Proposed by Yongjian and Acton [10], SRAD filter is an extension of AD filter by Perona and Malik in [9], aimed at being more efficient in speckle removing. It still operates based on diffusion PDE like AD filter but additionally utilizes ICOV [15]. ICOV is considered as the discriminating factor for edge detection and it becomes the determinant whether a pixel should be smoothed or not [16]. Fully developed coefficient variation can be represented as the ratio of noise standard deviation to noise mean:

$$q_0(t) = \frac{\sigma_n(t)}{\mu_n(t)}, \tag{7}$$

and ICOV is defined as:

$$q(x,y,t) = \sqrt{\frac{\frac{1}{2}(|\nabla \mathrm{I}|/I)^2 - \frac{1}{16}(\nabla I^2/I)^2}{(1+(\frac{1}{4})(\nabla I^2/I))^2}}, \tag{8}$$

The diffusion function $c(.)$ can be described as

$$c[q(x,y,t), q_0(t)] = \left(1 + \frac{q^2(x,y,t) - q_0^2(t)}{q^2(x,y,t)(1+q_0^2(t))}\right)^{-1} \tag{9}$$

2.1.3 NLM Filter

Non-local means filter uses non-local pixels in the filtering process. This is different than the concept of previous filters which are all based on local relevant pixels. Proposed by Buades in [12] this filter uses the approach of comparing non-local patches and based on their similarity filtering is conducted [17]. This is called the self-similarity concept which was first introduced by Efros and Leung [18]. The non local patches comparison process can further be explained by taking the examples as shown in Fig. 2.

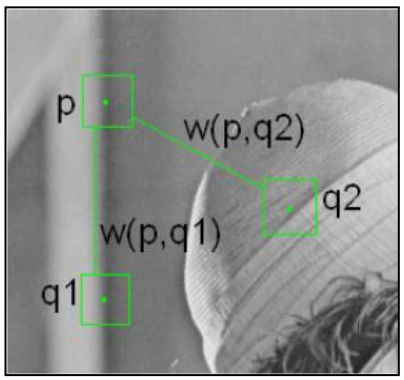

Figure 2: Depiction of self similarity concept, with pixels p, q1 and q2

As shown in Fig. 2, pixels p belongs to neighborhoods that are more similar to that of pixels q1 rather than pixels q2. Hence due to this, the denoised value of p will be more affected by q1 than q2. Similar neighborhoods result in greater weight,

w(p,q1) and different neighborhoods result in less weight w(p,q2). The noisy image given as $V(j)$ and $NL(V)(i)$ of pixel i is expressed as

$$NL(V)(i) = \sum_{j \epsilon V} \omega(i,j)\, V(j), \tag{10}$$

where weights $\omega(i,j)$ depends on similarity between pixels i and j with conditions $0 \leq \omega(i,j) \leq 1$ and $\omega(i,j)$ =1. The similarity of pixels i and j depends on the intensity gray level vectors of each corresponding neighborhood denoted as $V(N_i)$ and $V(N_j)$ where N_k represents square neighborhood centered by pixel k. Weighted sum of squared difference (ssd) between the neighborhoods is evaluated in order to match the similarity of the neighborhood [18]. Ssd is expressed as quotient

$$ssd(i,j) = ||V(N_i) - V(N_j)||^2_{2,\alpha}\,, \tag{11}$$

where α is the neighborhood filter. The weights can be written as

$$\omega(i,j) = \frac{1}{Z(i)} e^{-\frac{ssd\,(i,j)}{h^2}}, \tag{12}$$

and $Z(i)$ as

$$Z(i) = \sum_{j} e^{-\frac{ssd\,(i,j)}{h^2}}, \tag{13}$$

whereby $Z(i)$ is the normalizing constant and h is the degree of filtering.

2.1.4 LMMSE Wavelet Filter

Proposed by Zhang and Bao this filter is a LMMSE-based with optimal wavelet selection filter. The pioneer wavelet soft thresholding concept was proposed by Donoho, and afterwards followed by many other wavelet-based methods such as in [19], [20], and [21].

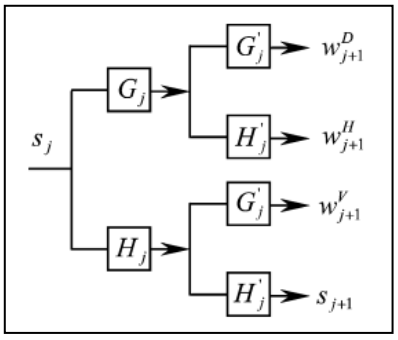

Figure 3: One stage decomposition of the 2-D OWE w_j^H, w_j^V and w_j^D are the wavelet coefficients at horizontal, vertical and diagonal directions

Zhang and Bao utilized the interscale model and presented using overcomplete wavelet expansion (OWE) described in Fig. 3 above [11]. Wavelet filters must have two characteristics in order to perform denoising which is the ability to extract signals from noisy wavelet coefficient and another is the resemblance of interscale image wavelet coefficients distributions to jointly Gaussian. M is defined based on the information of noiseless and noisy wavelet coefficients and it is proportional to the performance of the scheme [11]. E is the factor that evaluates the resemblance between the Gaussian and real signal density which is inversely proportional to the denoising performance. Optimal wavelet could be derived from a library of wavelets based on the M and E values of them [22].

2.2 Performance Metrics

This section analyzes several common performance metrics that are used to evaluate the performance of the despeckle filters. They measure the ability of denoising, image restoration, contrast enhancement and edge preservation. Some of these performance metrics are Mean Square Error (MSE), Peak Signal to Noise Ratio (PSNR), Signal to Noise Ratio (SNR), Normalized Variance, Effective Number of Looks (ENL), Contrast-to-Speckle Ratio (CSR), Mean Preservation and Ultrasound Despeckling Assessment Index (USDSAI) and Edge Preservation Index (EPI) [14]. They are expressed as:

$$MSE = \frac{1}{MN}\sum_{j=1}^{M}\sum_{k=1}^{N}(X_{j,k} - X_{j,k}^{'})^2, \tag{14}$$

where $X_{j,k}$ represents the original noisy image pixels and $X_{j,k}^{'}$ represents the denoised image pixels

$$PSNR = 10\log_{10}\frac{(2^n - 1)^n}{MSE}, \tag{15}$$

where PSNR is a ratio of maximum power of signal to the noise level. Lower normalized variance signifies better speckle reduction and it is expressed as

$$Normalized\ Variance = \frac{var}{mean^2} = \frac{\frac{1}{MN}\sum_{j=1}^{M}\sum_{k=1}^{N}(X_{j,k} - \bar{X})^2}{\bar{X}^2} \tag{16}$$

$$ENL = \frac{[NMV]^2}{[NSD]^2}, \tag{17}$$

where NMV stands for normalized variance and NSD normalized standard deviation.

$$CSR = \frac{((|\mu_1 - \mu_2|)\mu_1)}{\sqrt{(\sigma_1^2 + \sigma_2^2)}}, \tag{18}$$

CSR provides a measure of contrast level comparison between the original and restored images. $\mu_1, \mu_2, \sigma_1,$ and σ_2 are the mean and standard deviations of original and despeckled images respectively.

On the other hand Mean Preservation compares the mean intensity in original noisy image to the mean intensity of the restored images. The mean of restored images that has nearest value to mean of original image indicates that the filter has the best ability to retain the originality of the US image [23]. USDSAI measures the speckle filters' performance in terms of reduction in variances of homogenous regions while separating the different regions apart. Higher USDSAI values indicate better image restorations and better contrast preservation by the filter [23].

$$Mean\ Preservation\ \bar{X} = \frac{1}{MN}\sum_{j=1}^{M}\sum_{k=1}^{N} X_{j,k} \tag{20}$$

$$USDSAI = \frac{\sum_{k \neq l} mean_{C_k} - mean_{C_l}}{variance_{C_k}} \tag{19}$$

EPI will measure the filters' ability in terms of edge preservation.

$$EPI = \frac{|p_s(i,j) - p_s(i-1, i+1)|}{|p_o(i,j) - p_o(i-1, i+1)|} \tag{20}$$

MSE, PSNR, SNR, Normalized Variance and ENL are usually used to measure the filters' ability in speckle removal. CSR and EPI on the other hand are used for evaluating the filters' performance in contrast level and edge preserving capabilities respectively [24]. Mean preservation is used to check the filters' ability in retaining image originality while USDSAI evaluates image restoration capability.

2.3 Related Works

Various studies have been conducted to evaluate the performance of the filters in order to determine which methods are more superior in terms of speckle removal and edge preservation. Most studies however, reveal that it is difficult to achieve both standards because they are somehow contradicting [15].

In [25], Runxia et. al made comparison study between SRAD, Kuan, NLM, Frost and Homomic filters. The performances of the filters are evaluated using six different performance evaluation metrics, Least Absolute Error (LAE), Figure of Merit (FOM), SNR, CNR, S/MSE and EPF. The denoising process is conducted using Lena image which is introduced with noise and ultrasound image liver. From the study, it was discovered that SRAD is most capable in denoising and preserving edges as it has the highest SNR and EPI.

Wanjun et. al makes performance evaluation study of a few filters namely, Lee, wavelet shrinkage, SRAD, GenLik, NLM and NLM with multi-shape patches aggregation (NLM-MSPA) [17]. NLM-MSPA is proposed by the researchers in this study which is designed as extension of the classical NLM. However, this paper evaluates the filters in terms of speckle removal only measured by SNR values. The despeckling filters are applied to MRI gastrointestinal image corrupted with noise and real abdominal aortic aneurysm US image. The study proves that the NLM-MSPA is most competitive obtaining the largest SNR value. SRAD outperforms original NLM having higher SNR values.

CHAPTER 3

METHODOLOGY

The experiments will be carried out using 3 different types of images namely simulated noise image, computer generated US image and real US images. The computer generated US image is generated using software called Field II Simulator. The sequential steps can be observed in the flowcharts below:

3.1 Using Simulated Noise Speckled Images

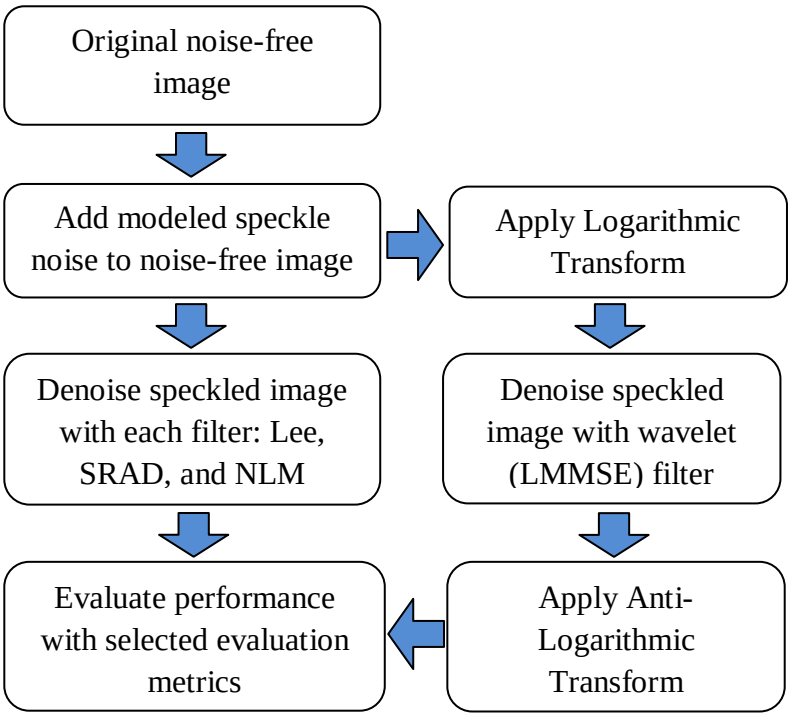

3.2 Using Computer Generated Image

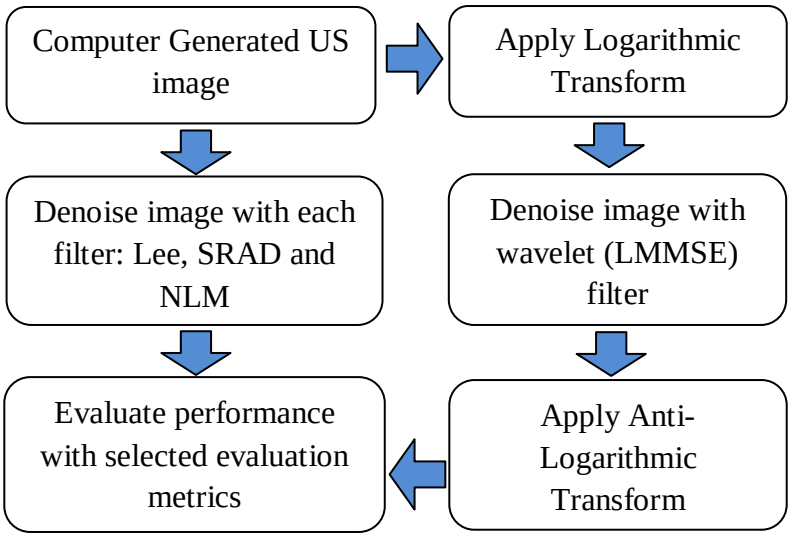

3.3 Using Real US Image

Real US image is obtained and to be downloaded from INSANA Lab website.

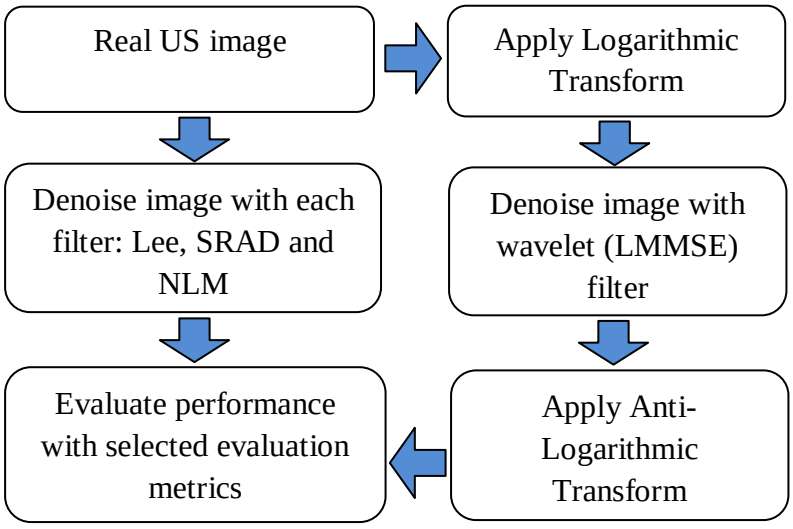

Logarithmic transform is performed everytime before the speckled image is despeckled by wavelet (LMMSE) filter in order to convert multiplicative noise to additive noise. This is to suit the property of the wavelet filter that is designed for additive noise [11]. Therefore, as shown in the flow charts the denoised images are converted back to non-logarithmic form before evaluated using selected performance metrics.

3.3 Selected Performance Evaluation Metrics

In this paper, the performance metrics that are selected to be used are PSNR, Normalized Variance, USDSAI and Mean Preservation. PSNR and Normalized Variance will measure the filters' effectiveness in terms of noise removal while USDSAI evaluates the ability of the filters in terms of image restorations. Mean Preservation will evaluate the performance of the filters in terms of their ability to maintain the image features. In the first part of experiment where simulated speckled noise images are used, PSNR and USDSAI evaluations are made. USDSAI evaluations are made over a few selected regions from the images. As for the second and third part of the experiment where computer generated images and real US images are utilized, Normalized Variance, USDSAI and Mean Preservation evaluations are carried out. Similar to USDSAI evaluations Normalized Variance and Mean Preservation are also evaluated over selected regions. This will be further discussed in the next chapter which encloses results and discussions part.

CHAPTER 4

RESULTS & DISCUSSIONS

4.1 Using Simulated Noise Speckled Image

In this section, the results of PSNR and USDSAI evaluations on the despeckled simulated noisy images are disclosed. Three images Lena, Barbara and Boat of size 128x128 shown in Fig. 4(a), (b) and (c) are used in the experiment of PSNR and USDSAI evaluations.

(a) (b) (c)

Figure 4: (a) Lena, (b) Barbara, (c) Boat image

4.1.1 PSNR and USDSAI Evaluations

The clean 128x128 images of Lena, Barbara and Boat are introduced with simulated speckle noise of varying noise variance levels. The comparisons of PSNR values are shown in Table 2. The USDSAI was evaluated over three regions named region A, B and C. The selected regions are shown in Fig. 5 for Lena, Barbara and Boat respectively. The comparisons of USDSAI values are depicted in Table 3.

(a) (b) (c)

Figure 5: (a) Lena, (b) Barbara and (c) Boat with their selected regions for USDSAI evaluation

Table 2: Comparison of PSNR values for each denoising filter on speckled images

Lena									
Method		Noise standard variance, σ							
		0.04	0.06	0.08	0.1	0.2	0.3	0.4	0.5
PSNR	Noisy	27.20	25.44	24.18	23.22	20.22	18.47	17.19	16.24
	SRAD	24.33	22.66	21.03	19.30	16.41	14.07	13.54	12.62
	Lee	26.11	25.94	25.78	25.66	25.13	24.71	23.70	23.19
	LMMSE	**28.58**	**28.70**	**28.76**	**28.67**	**28.08**	**27.02**	**24.32**	**22.47**
	NLM	27.75	27.64	27.54	27.39	26.57	25.59	23.20	21.83
Barbara									
Method		Noise standard variance, σ							
		0.04	0.06	0.08	0.1	0.2	0.3	0.4	0.5
PSNR	Noisy	25.99	24.24	22.95	22.04	18.99	17.24	15.99	15.02
	SRAD	18.74	17.61	16.01	15.48	13.60	13.27	10.84	10.80
	Lee	23.22	23.08	22.92	22.70	22.16	21.63	21.14	20.68
	LMMSE	24.53	24.58	24.63	24.67	**24.46**	**23.69**	**22.33**	**20.84**
	NLM	**25.29**	**25.22**	**25.09**	**25.01**	23.95	22.54	21.09	19.72
Boat									
Method		Noise standard variance, σ							
		0.04	0.06	0.08	0.1	0.2	0.3	0.4	0.5
PSNR	Noisy	25.41	23.65	22.42	21.44	18.44	16.67	15.44	14.47
	SRAD	21.61	20.34	18.44	16.96	14.08	12.75	11.54	10.67
	Lee	22.11	22.11	22.0	21.87	21.36	20.89	20.45	20.07
	LMMSE	**24.40**	**24.74**	**24.77**	**24.79**	**24.67**	**23.80**	**22.35**	**20.72**
	NLM	24.33	24.31	24.30	24.25	23.64	22.42	21.40	19.71

Table 3: Comparison of USDSAI values for each denoising filter on speckled images

Lena									
Method		Noise standard variance, σ							
		0.04	0.06	0.08	0.1	0.2	0.3	0.4	0.5
PSNR	Original	1	1	1	1	1	1	1	1
	Noisy	0.89	0.81	0.76	0.79	0.60	0.55	0.43	0.36
	SRAD	1.06	1.04	0.98	1.07	1.39	1.26	**1.32**	0.79
	Lee	1.30	1.25	1.19	1.32	1.20	1.22	1.14	**0.93**
	LMMSE	1.27	1.21	1.15	1.26	1.18	1.10	0.95	0.72
	NLM	**1.52**	**1.46**	**1.43**	**1.52**	**1.44**	**1.35**	1.28	0.92
Barbara									
Method		Noise standard variance, σ							
		0.04	0.06	0.08	0.1	0.2	0.3	0.4	0.5
PSNR	Original	1	1	1	1	1	1	1	1
	Noisy	0.93	0.84	0.79	0.71	0.71	0.52	0.55	0.44
	SRAD	1.07	0.96	0.87	0.84	0.91	0.70	0.70	0.79
	Lee	1.38	1.28	1.24	1.17	1.38	1.04	1.34	1.08
	LMMSE	1.12	1.08	1.06	0.99	1.22	0.88	1.08	0.83
	NLM	**1.64**	**1.56**	**1.50**	**1.46**	**1.57**	**1.18**	**1.49**	**1.15**
Boat									
Method		Noise standard variance, σ							
		0.04	0.06	0.08	0.1	0.2	0.3	0.4	0.5
PSNR	Original	1	1	1	1	1	1	1	1
	Noisy	0.87	0.75	0.83	0.74	0.69	0.54	0.49	0.37
	SRAD	1.01	1.11	1.28	1.16	1.14	1.09	1.05	1.04
	Lee	1.44	1.27	1.44	1.34	1.52	1.37	1.14	1.06
	LMMSE	1.26	1.14	1.29	1.19	1.39	1.22	1.02	0.84
	NLM	**1.70**	**1.61**	**1.79**	**1.67**	**1.66**	**1.59**	**1.24**	**1.10**

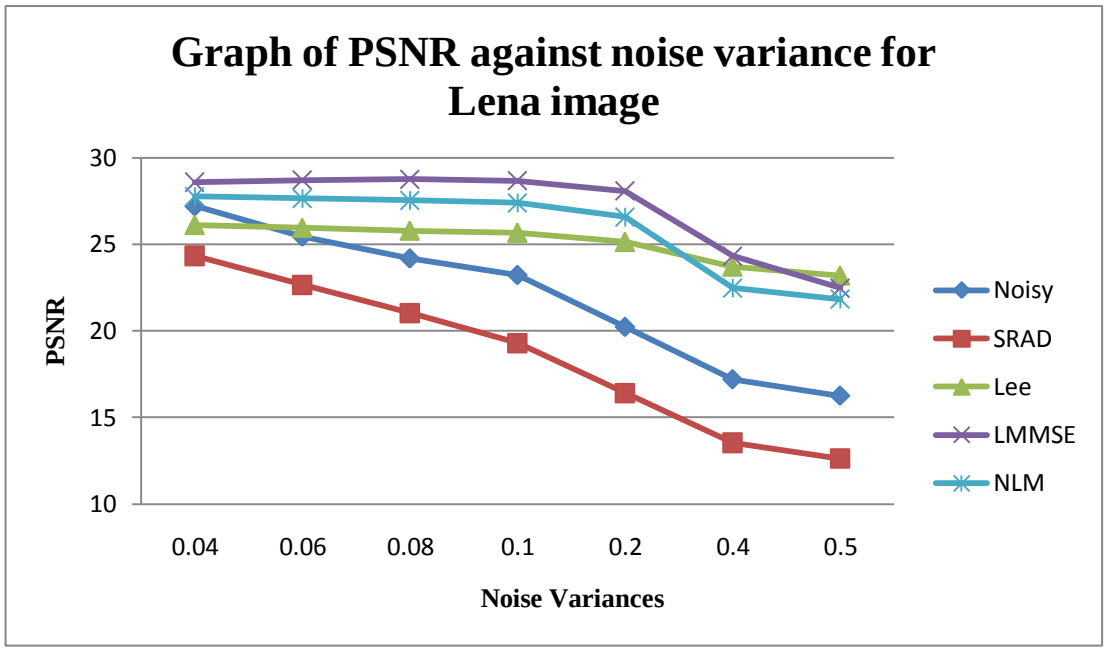

Graph 6: PSNR against noise variance for Lena image

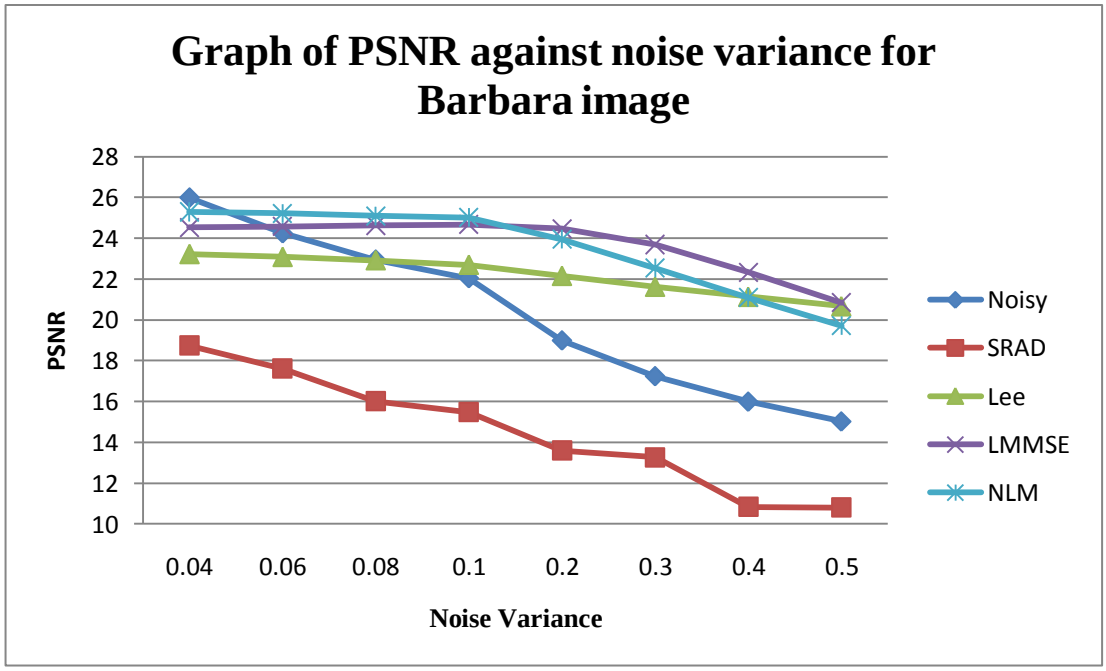

Graph 7: PSNR against noise variance for Barbara image

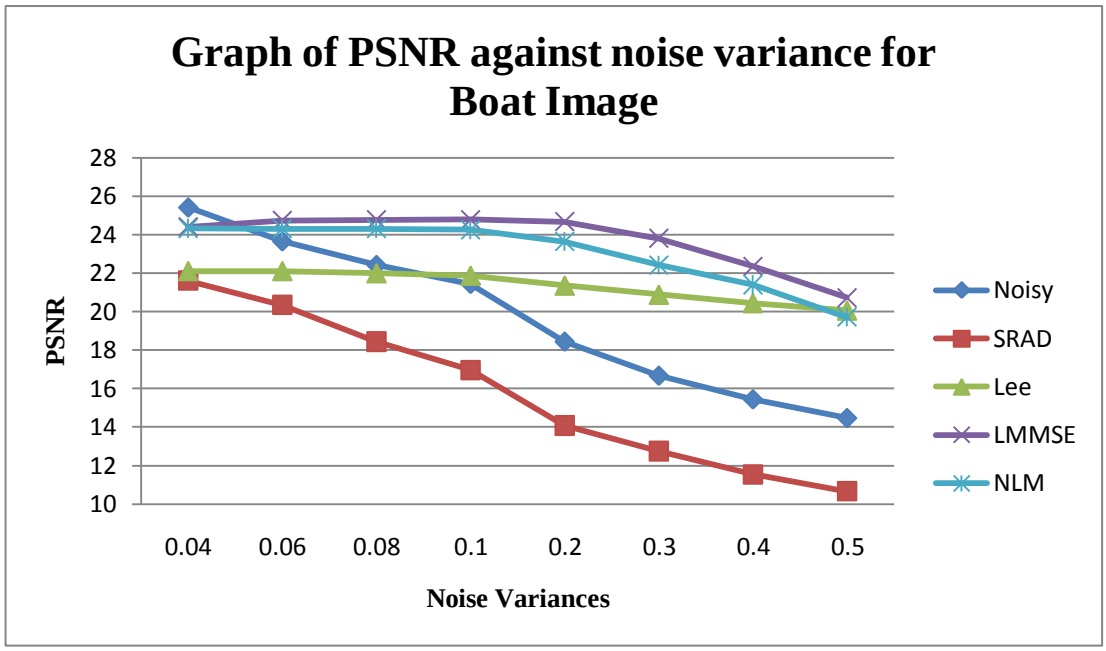

Graph 8: PSNR against noise variance for Boat Image

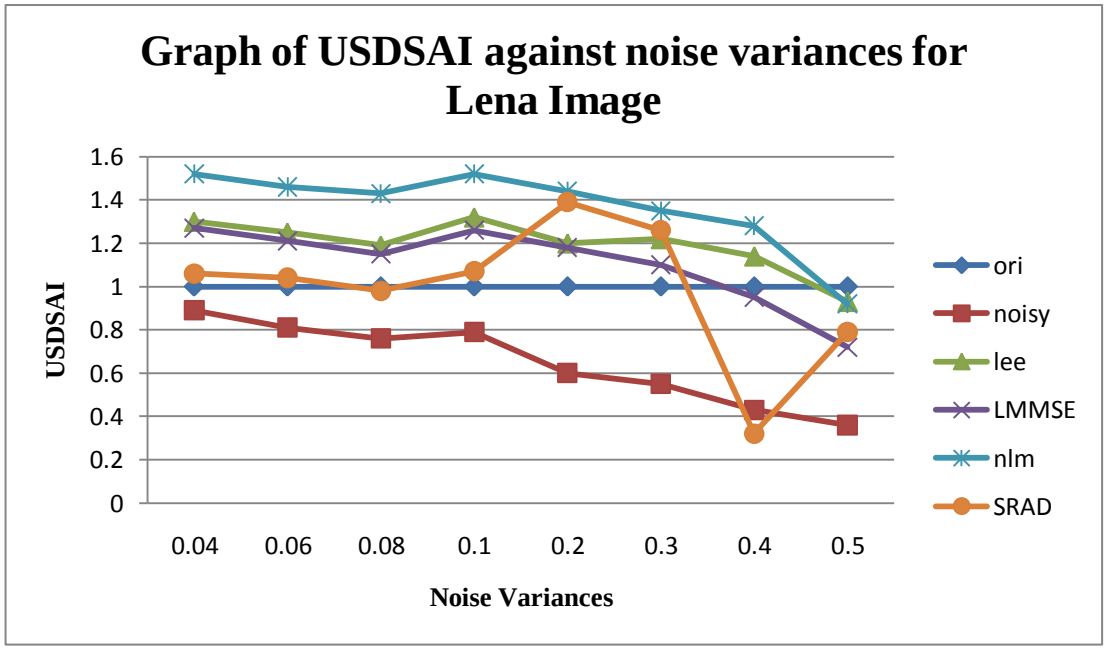

Graph 9: USDSAI against noise variance for Lena Image

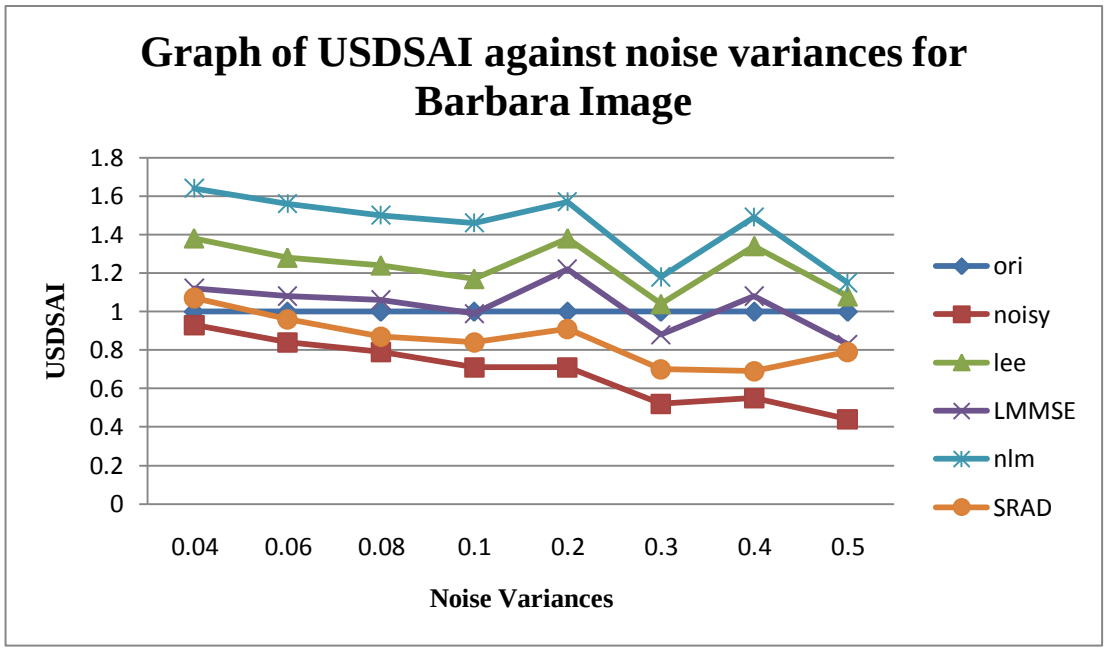

Graph 10: USDSAI against noise variances for Barbara Image

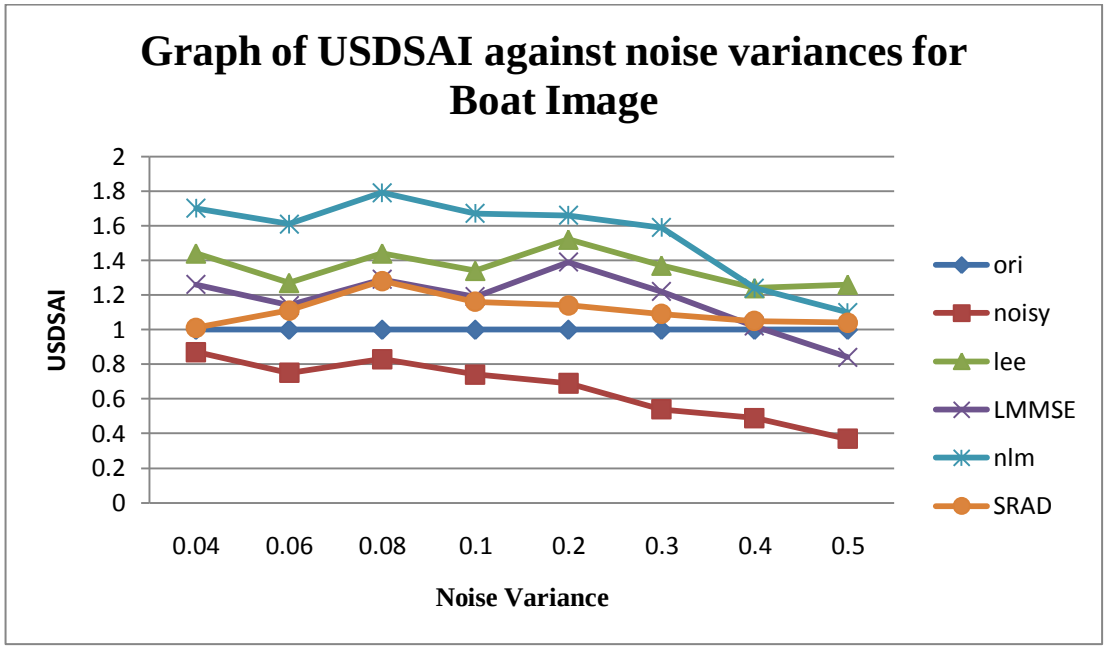

Graph 11: USDSAI against noise variances for Boat Image

From the results depicted in Table 2 and Graph 1 it is evident that wavelet (LMMSE) is the most superior despeckling technique with the highest PSNR values which are underlined and bolded in the Table 2. The average gain of PSNR values for wavelet (LMMSE) method is 5.56 dB for Lena image. This is followed by NLM filter with average gain of PSNR 4.42 dB and then Lee with average gain of PSNR by 3.51 dB. Since SRAD filter has negative average gain of PSNR the values are dismissed. It is observed that the PSNR values decrease as the noise level increases and this is true for each filter especially for SRAD which is extremely sensitive to increase in noise level. Eventhough NLM filter gives a higher average gain of PSNR compared to Lee filter it is more sensitive to increase in noise level resulting in lower PSNR value (PSNR=21.83) at noise variance 0.5 as compared to Lee filter (PSNR=23.19).

In terms of USDSAI assessment, it can be seen from Table 3 and Graph 4 that NLM filter performs best for Lena with highest USDSAI values at noise variances from 0.04 up to 0.3. There is a slight irregularity for the result data at noise variance 0.4 and 0.5 whereby the highest USDSAI values at these variances are by SRAD and Lee filters respectively. However, it can be considered that NLM outperforms other filters since it gives highest USDSAI readings for majority of noise variances. The USDSAI values are consistently higher than 1 which means the restored images are improved in terms of contrast. The higher USDSAI values by NLM filter indicates that this filter provides desirable image restoration and preserves contrast.

In terms of visual assessment, it can be seen in Fig. 6(c) that SRAD filter does not result in over-smoothing and hence does not cause blurring. However it can be observed that there are still a lot of speckle retained in the image. Lee filter utilized in this experiment is of window size 3 by 3 and the despeckled Lena image by Lee is shown in Fig. 6(d). Lee filter performs well in terms of noise removal whereby almost 70% of the speckle noise is removed. However the filtering results in blurring effect and failure in preserving the edges as well as important features of the image. This is evident for instance, focusing on the furry part of Lena's hat in Fig. 6(d) which has become blurry and indistinct. Wavelet (LMMSE) performs extremely well in removing the speckle noise which can be analyzed in Fig. 6(e) whereby the image seems almost clear from noise and just a slight remaining noise left. It does result in blurring to some degree though much less than in Lee filter. The furry part

of the hat is still visible and distinguishable in Fig. 6(e) therefore it can be said that wavelet (LMMSE) is able to preserve edges and textures in an image. NLM filter also did a good job in terms of speckle noise suppression however it causes more blurring than wavelet (LMMSE) filter.

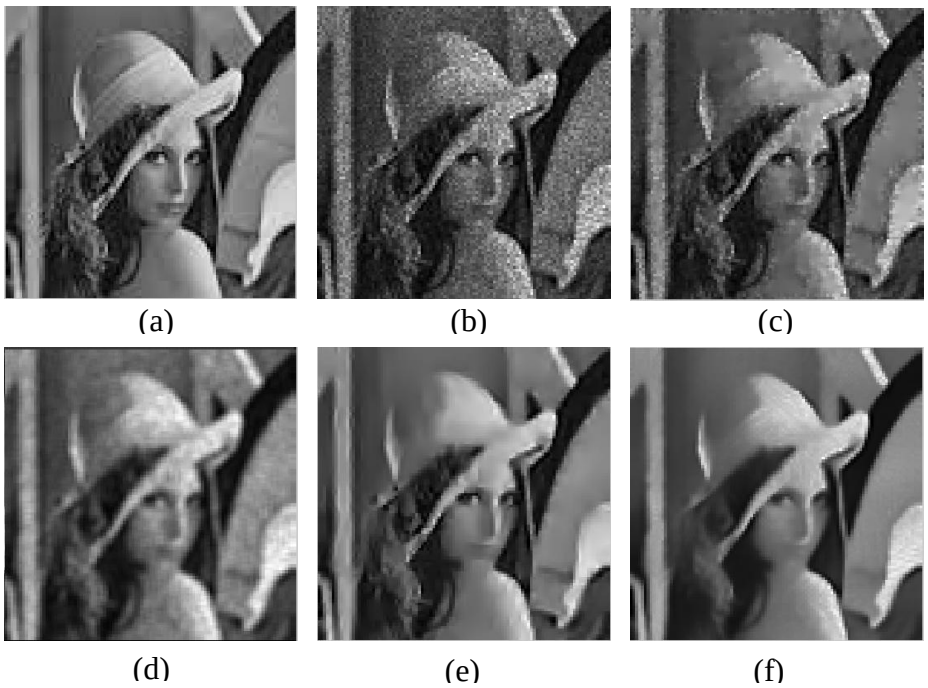

Figure 6: Lena images with noise variance 0.1. (a) Noise-free image (b) Noisy image (c) SRAD Filter (d) Lee Filter (e) LMMSE Filter (f) NLM Filter

As for Barbara image, the results for PSNR values are as per tabulated in Table 2 and translated in Graph 2. It is seen that NLM filter has the highest PSNR values for noise variance 0.04 up to 0.1 but starting from noise variance 0.2 up to 0.5 wavelet LMMSE filter is seen to be having highest USDSAI values. The average gain of PSNR of wavelet (LMMSE) is 3.41 dB, whereas for NLM is 3.18 dB and Lee with 1.88 dB. The SRAD filter gives negative gain throughout all the noise levels. The highest average gain PSNR is apparently from wavelet (LMMSE) followed by NLM and then Lee. It is also analyzed that it is similar as in Lena image, whereby the filters' PSNR values decrease as the noise level increases. Lee filter is the least affected by the noise level while SRAD filter is the most susceptible to increment of noise levels. Eventhough NLM filter performs well with lower noise variance the performance starts to decline with higher noise variance. At noise variance 0.5 Lee filter is observed to have higher PSNR value than NLM filter.

On the other hand in terms of USDSAI evaluations for Barbara image, it is shown in Table 3 and Graph 5 that NLM filter produces highest values at all noise variances consistently. Based on observations from Graph 5 the ranking is followed by Lee, wavelet LMMSE and SRAD filters. Therefore based on the USDSAI evaluation it can be said that NLM filter produces desirable image restoration for Barbara image.

For visual evaluation, referring to Fig. 7(c) it is observed that SRAD filter did not perform denoising well enough since the image is still highly corrupted with noise. Fig. 7(d) shows the despeckled image by Lee filter which contains less noise but very blurry. This is evident since the tablecloth chequered pattern is not visible in Fig. 7(d). Lee filter did a good job at removing speckle noise however performs poorly in retaining the features and details of image as well as preserving the edges. It is shown in Fig. 7(e) that wavelet (LMMSE) filter performs very well in terms of speckle noise suppression but leads to over-smoothing in some parts of the image. The image is quite blurry but some of the important features are still retained such as the tablecloth chequered pattern is still distinguishable in the image. The same can be concluded for the image in Fig. 7(f) which depicts the result from NLM filter whereby the image is almost the same as in Fig. 7(e). The difference is however, it is slightly more blurry than the image filtered by wavelet (LMMSE) filter, where it can be seen that Barbara's face is less visible compared to in Fig. 7(e). Therefore it can be stated that both wavelet (LMMSE) and NLM filter are competent in terms of speckle noise suppression but wavelet (LMMSE) filter is better at preserving edges than NLM filter.

Figure 7: Barbara images with noise variance 0.1 (a) Noise-free image (b) Noisy image (c)SRAD Filter (d) Lee Filter (e) LMMSE Filter (f) NLM Filter

In Boat image, the results for PSNR values are as per tabulated in Table 2 and illustrated in Graph 3. The wavelet (LMMSE) filter performs best by having the highest PSNR values as shown underlined and bolded in Table 2. The average gain of PSNR of wavelet (LMMSE) is 4.04 dB, NLM with 3.30 dB and Lee with 1.62 dB. The SRAD filter gives negative gain throughout all the noise levels. The highest average gain PSNR is clearly from wavelet (LMMSE) followed by NLM and then Lee. The filters' PSNR values decrease with increasing noise level.

In terms of USDSAI assessment, it can be seen from Table 3 and Graph 6 that once again NLM filter shows the highest USDSAI values. The USDSAI values are consistently higher than 1 (except at noise variance 0.4 and 0.5) hence the restored images are improved compared to original unprocessed image in terms of contrast. Thus this indicates that NLM filter is best in noise reduction while maintaining the image contrast.

The visual inspection for Boat image also reveals almost similar conclusions as in Lena and Barbara images. Fig. 8(c) shows the boat image denoised by SRAD filter which can be seen very noisy still. Eventhough the image details are not

smoothed out to the point of blurring however the noise removal is not up to satisfactory level. In Fig. 8(d) it is depicted that Lee filter removes some speckle noise but the image is still noisy and on top of that the image is blurry with low clarity. On the other hand in Figs. 8(e) and 8(f) it can be scrutinized that both wavelet (LMMSE) and NLM filters denoise the images very well as the images produced are almost free from speckle noise. Both of these images highly resemble the original noise-free image, but some of the features are smoothed and blurred to some extent. Hence for boat image, it can be said that both wavelet (LMMSE) and NLM filters are competent in terms of speckle noise reduction and maintaining the edges and textures of image.

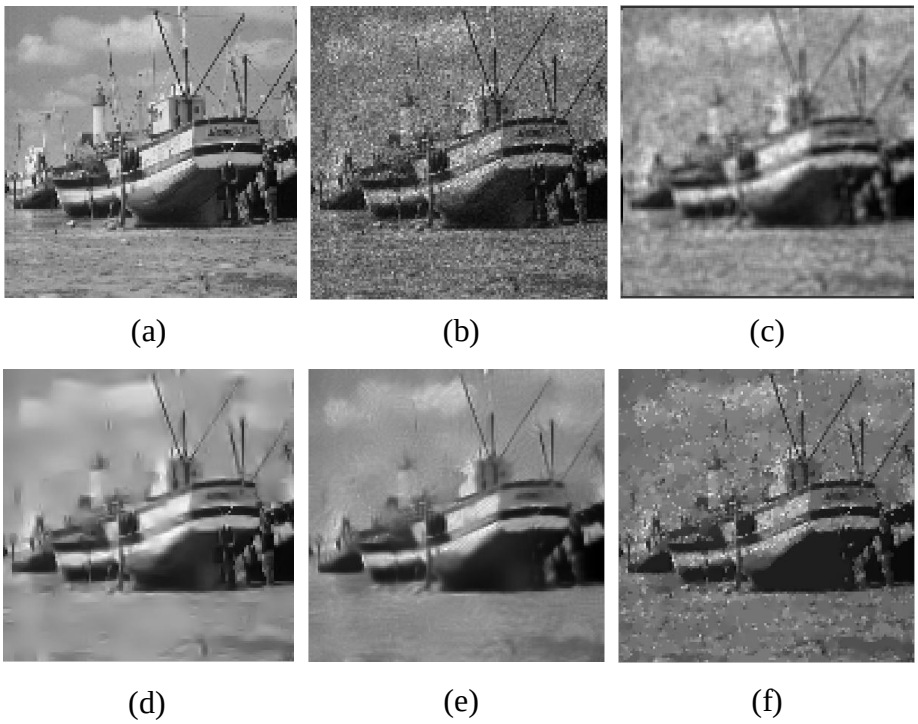

Figure 8: Boat images with noise variance 0.1. (a) Noise-free image (b) Noisy image (c) SRAD Filter (d) Lee Filter (e) LMMSE Filter (f) NLM Filter

4.2 Using Field II Simulated Image

In this part of experiment, a cyst resembling phantom image is generated using the MATLAB Field II simulation version 3.2. The cyst phantom image generated is as shown in Fig. 9. The y-axis shows the axial size while the x-axis shows the lateral size. The phantom consists of five point targets; 6, 5, 4, 3, and 2 mm diameter water-filled cysts, along with 6, 5, 4, 3, and 2 mm diameter high scattering regions. Essentially, the phantom is composed of 3 constant classes and the filters' ability to reduce speckle noise while keeping the distinct classes well separated will be

evaluated using USDSAI assessment. The results for USDSAI, normalized variance, and mean preservation can be analyzed in Fig. 10, Table 4 and Table 5 respectively. Before the image is despeckled, it is resized to 256x256 in order to allow it to be processed by all filters.

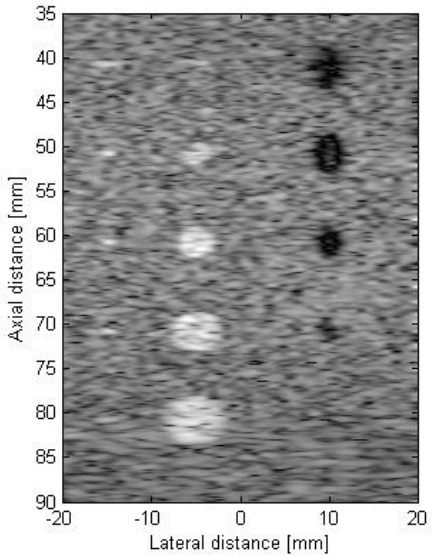

Figure 9: Field II Simulated Image, Cyst Phantom

As mentioned earlier, USDSAI evaluation is carried out for cyst phantom image. Hence three regions region A, B and C are selected for the USDSAI evaluation and they are presented in Fig. 10(a). The USDSAI values for each filter are shown together with the denoised images in Fig. 10(b), (c), (d) and (e).

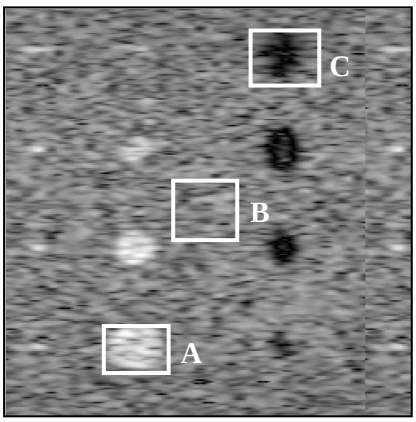

(a) USDSAI=1.00

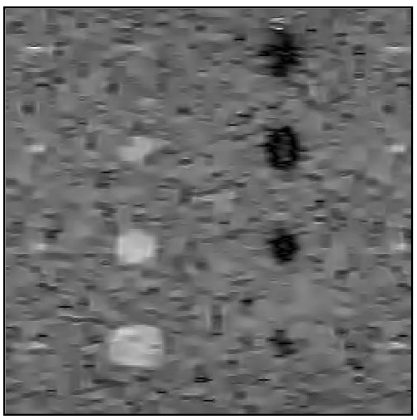

(b) USDSAI=1.22

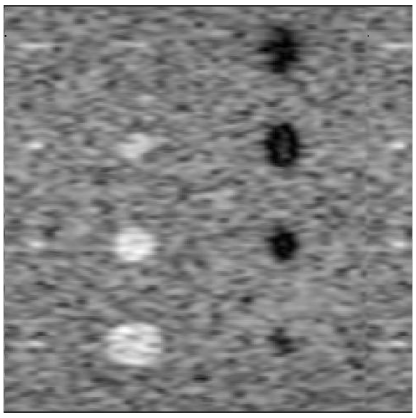

(c) USDSAI=1.34

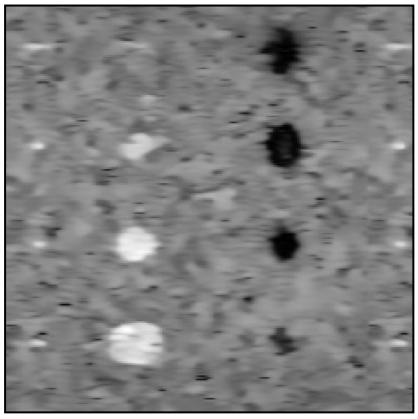

(d) USDSAI=1.50

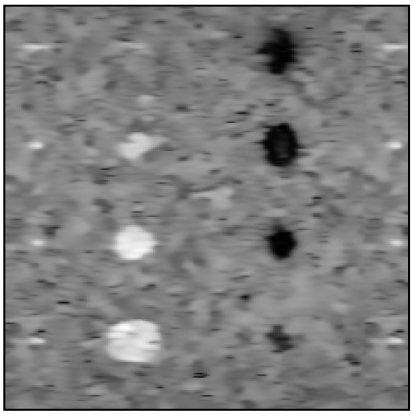

(e) USDSAI=1.33

Figure 10: Field II Simulated Image, Cyst Phantom with respective USDSAI values (a) original image (b) wavelet LMMSE filter (c) Lee filter (d) NLM filter (e) SRAD filter

The normalized variance and mean preservation are calculated over two regions and in this report the regions used are called region A and region B. Regions A and B for this part of experiment is the same as the regions A and B selected earlier for USDSAI assessment. The results for normalized variance and mean preservation are disclosed in the following tables.

Table 4: Normalized Variance for restored images in Fig. 9

Regions	Original	SRAD	Lee	LMMSE	NLM
A	0.0473	0.0364	0.0359	0.0362	0.0359
B	0.0417	0.0200	0.0259	0.0292	0.0140

Table 5: Mean Preservation for restored images in Fig. 9

Regions	Original	SRAD	Lee	LMMSE	NLM
A	178.34	0.70	178.40	177.38	178.32
B	128.27	0.50	128.19	127.02	129.71

From the result obtained for USDSAI evaluation the highest USDSAI value achieved is 1.50 by NLM filter. This is followed by Lee, SRAD and then wavelet LMMSE. However all the restored images are improved in terms of contrast level since all of them have USDSAI values greater than 1. Therefore for Field II simulated image, NLM filter is proven to be better and produces more desirable image restoration.

Normalized variance and mean preservation of the original cyst phantom image are calculated and compared to the normalized variance and mean preservation of all restored images by each filter. The reduction of normalized variance in denoised image indicates better noise reduction by the filter. From Table 4 it is evident that NLM filter results in lowest normalized variance in both region A and B hence indicating high level of noise reduction. This is followed by Lee, SRAD and wavelet LMMSE. Through mean preservation aspect, for region A it is observed in Table 5 that NLM is best at preserving mean as the restored image by this filter has closest mean to the original image's mean. However for region B, Lee is seen with closest mean value to the original image's mean value. This is probably due to the nature of Lee filter that is based on averaging technique hence it has the tendency to retain the mean of original image.

Through visual inspection, the restored images by SRAD filter in Fig. 10(e) are much less noisy than the original however it suffers some loss in details and textures as the filter tends to smooth the image. Lee filter reduces speckle noises but it causes blurring effect to the denoised image making it difficult to be analyzed. NLM filter performs best for Field II simulated image since it is excellent at removing noise and still manages to maintain the image details, textures and enhances contrast as confirmed by its highest USDSAI value. The restored image by SRAD is over-smoothed and the image details and textures are lost.

4.3 Using Real US Images

In this part of experiment, the performances of the filters are analyzed using real ultrasound images captured from patients. The images used are malignant and benign tumor shown in Fig. 11 (a) and (b) accordingly. The image size is 1536 × 256 pixels. In Fig. 11, the patient with malignant tumor was diagnosed with IDC (Invasive Ductal Carcinoma) and the patient with benign tumor was diagnosed with fibroadenoma. The RF frames are recorded at 17 frame/second and a total of 12 seconds of data are obtained using a linear transducer array from the Antares ® System. The URI Offline Processing Tools (URI-OPT) run on MATLAB platform is used to convert the RF data to the B-mode images as shown in Fig. 10. The performances of filters in denoising real US images are evaluated through USDSAI, mean preservation and normalized variance. For USDSAI assessment to be carried out, three regions are selected regions A, B and C for both benign and malignant tumor image. The restored images for benign tumor are depicted in Fig. 12 along with the USDSAI results while the restored images for malignant tumor can be seen depicted in Fig. 13 together with the respective USDSAI values. The mean preservation and normalized variance are evaluated over two homogenous areas. The homogenous areas selected for benign tumor image are the corresponding regions A and C selected for USDSAI evaluation. Meanwhile for malignant tumor image, the homogenous areas chosen for mean preservation and normalized variance assessment are the corresponding regions A and B selected for USDSAI evaluation. Normalized variance and mean preservation results are presented in Table 6 and 7.

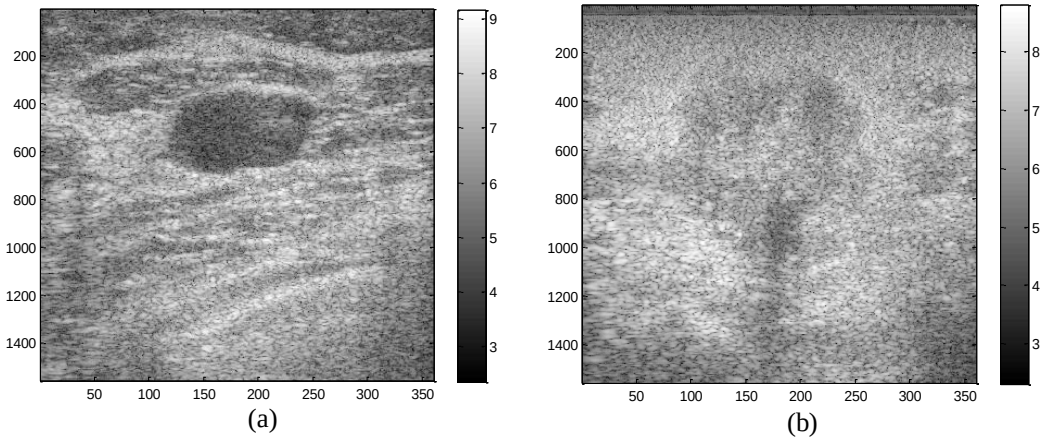

Figure 11: (a) benign tumor image (b) malignant tumor image of breast tissue

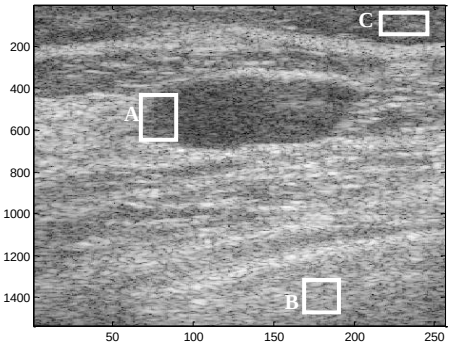

(a) USDSAI=1.00

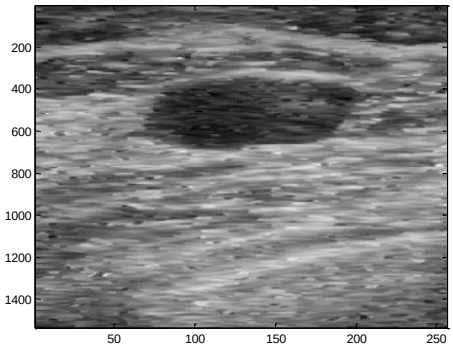

(b) USDSAI=6.52

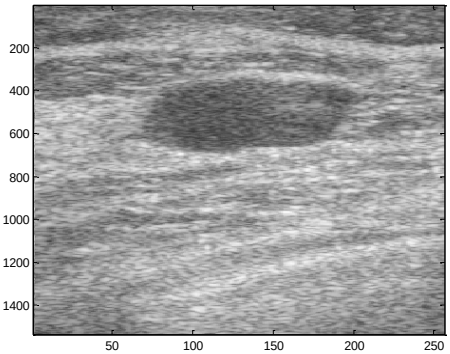

(c) USDSAI=3.42

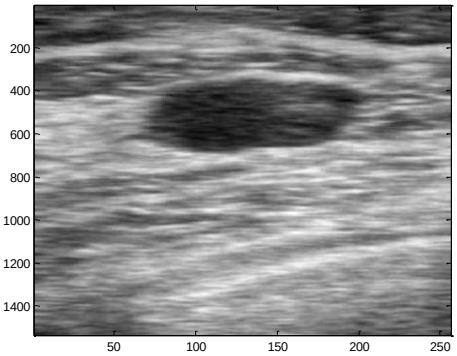

(d) USDSAI=10.02

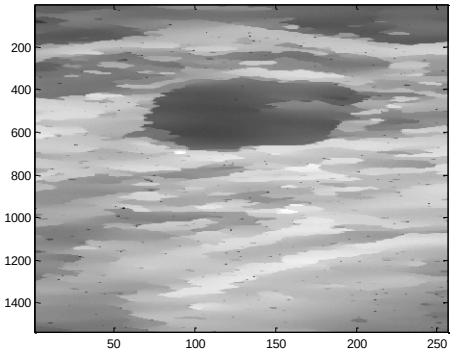

(e) USDSAI=5.17

Figure 12: Restored benign tumor images with USDSAI values(a) original (b) wavelet LMMSE filter (c) Lee filter (d) NLM filter (e) SRAD filter

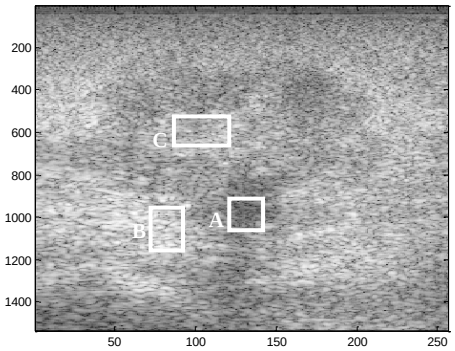

(a) USDSAI=1.00

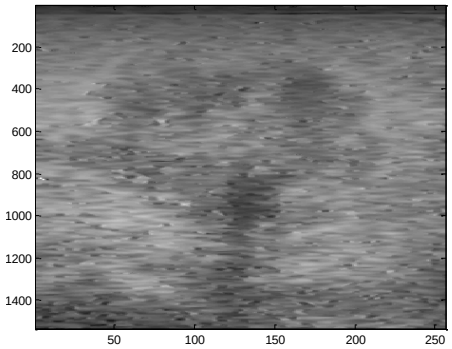

(b) USDSAI=7.32

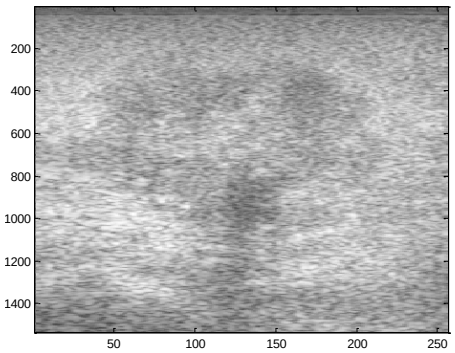

(c) USDSAI=5.05

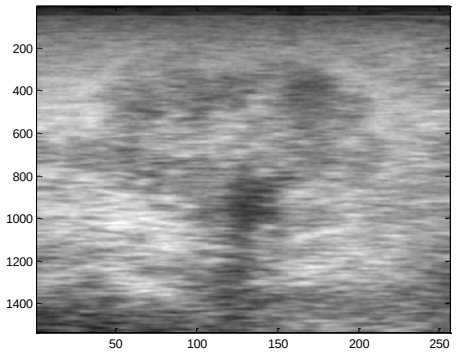

(d) USDSAI=8.97

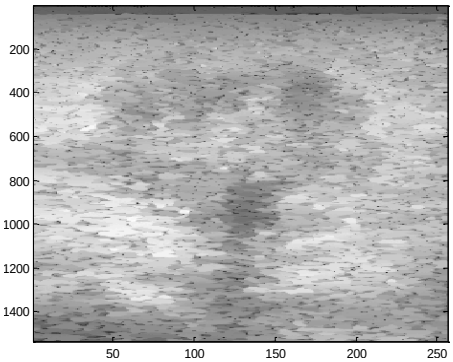

(e) USDSAI=6.45

Figure 13: Restored malignant tumor images with USDSAI values (a) original (b) wavelet LMMSE filter (c) Lee filter (d) NLM filter (e) SRAD filter

Table 6: Normalized Variance for restored images in Fig. 11 (benign tumors) and Fig. 12 (malignant tumors)

Benign Tumor	Original	SRAD	Lee	LMMSE	NLM
Region A	0.034	0.0039	0.0082	0.0040	0.0025
Region C	0.018	0.0048	0.012	0.0077	0.0044
Malignant Tumor	Original	SRAD	Lee	LMMSE	NLM
Region A	0.013	0.013	0.0067	0.0035	0.0021
Region B	0.0070	0.0097	0.0066	0.0039	0.0027

Table 7: Mean Preservation for restored images in Fig. 11 (benign tumors) and Fig. 12 (malignant tumors)

Benign Tumor	Original	SRAD	Lee	LMMSE	NLM
Region A	5.66	0.37	4.83	4.80	4.84
Region C	5.27	0.43	5.23	5.21	5.24
Malignant Tumor	Original	SRAD	Lee	LMMSE	NLM
Region A	6.90	0.47	5.29	5.27	5.32
Region B	7.18	0.80	7.49	7.49	7.47

From the results tabulated in Table 6 it is evident that the image denoised by NLM filter has lowest normalized variance indicating highest noise reduction. This is measured against the normalized variance of the original image before being denoised. This result is unanimous between both benign and malignant tumor images. As for benign tumor image the next best noise reducing filter is SRAD followed by wavelet LMMSE and Lee filter. Meanwhile, for malignant tumor image the next best noise reducing filter after NLM filter is wavelet LMMSE, followed by Lee and SRAD.

Table 7 shows the tabulated data of mean preservation for benign and malignant tumor images. It is shown that NLM filter results in mean value nearest to the mean value of original image before being denoised. This is then followed by Lee, wavelet LMMSE and SRAD. This is unanimous for both the benign and malignant tumor images. Fig. 12 and Fig. 13 show the restored benign tumor images and malignant tumor images together with their corresponding USDSAI values respectively. It is clearly shown from Fig.12 and 13 that wavelet LMMSE has significantly reduced noise while maintaining most of the image details. This is also supported by its high value of USDSAI. However the highest USDSAI value is found to be from the image denoised by NLM filter. Through visual inspection though, the image restoration by

NLM filter is slightly blurry compared to the image filtered by wavelet LMMSE. Nevertheless, the higher USDSAI value by NLM filter proves that it produces most desirable image restoration. SRAD filter produces over-smoothed image and Lee filter performs averagely in terms of USDSAI evaluation.

The processing times for each filter are also calculated and compared in Table 8. The time is measured in seconds.

Table 8: Processing time for each filter

	SRAD	Lee	LMMSE	NLM
Benign Tumor	63.98	82.33	65.99	671.66
Malignant Tumor	63.73	81.31	69.81	642.82

The filter with fastest processing time is SRAD filter which is then followed by wavelet LMMSE filter. Wavelet LMMSE is just slightly slower than SRAD. Lee filter has moderate processing time which is slower when compared to SRAD and wavelet LMMSE. NLM filter has the slowest processing time which is approximately 10 times the processing time for SRAD and wavelet LMMSE.

CHAPTER 5

CONCLUSION & RECOMMENDATIONS

This study focuses on the evaluation of the selected filters in terms of speckle noise suppression and texture preservation. The conducted experiments involved simulated speckled noise images, computer generated images and real US images. Using simulated data it is found that the wavelet LMMSE filter performs best in noise suppression as proven through PSNR assessment whereas NLM filter is the second best filter in terms of PSNR evaluation and it is as good as wavelet LMMSE filter. NLM filter is also competent in terms of producing desirable image restoration and this is proven through its USDSAI values. Using computer generated data and real ultrasound data, the NLM filter outperforms others in terms of USDSAI, mean preservation and normalized variance assessments. The processing time of NLM filter is the longest which is approximately 10 times the processing time for SRAD and wavelet LMMSE filters. The filter with next best performance but with faster processing time is wavelet LMMSE. It is concluded that NLM filter is the best filter in all scenarios considering both speckle noise suppression and image texture preservation.

A few recommendations are suggested to improve this work such as evaluating the performance of the filters with more performance metrics and using additional test images to be experimented on. Evaluation with more performance metrics will increase the accuracy of the result as the results will be more diverse. Using more test images will improve the results because different images produce unique results as such can be seen with the three different images used in this report.

CHAPTER 6

GANTT CHART, KEY MILESTONE AND STUDY PLAN

FYP 1

Key Milestones	Week													
	1	2	3	4	5	6	7	8	9	10	11	12	13	14
Selection of FYP title														
Project Planning														
Research and Literature Review														
Submission of Extended Proposal														
MATLAB development														
Proposal Defense														
Submission Draft of Interim Report														
Submission of Interim Report														
Result with noise simulated images														

Milestones

Process

GANTT CHART, KEY MILESTONE AND STUDY PLAN

FYP 2

Key Milestones	Week													
	1	2	3	4	5	6	7	8	9	10	11	12	13	14
Project Work Continues	■	■	■	■	■	■	■							
Submission of Progress Report							★							
Results with Computer Generated Image and Real US Image								■	■	■	■	★		
Pre-SEDEX										★				
Submission Draft of Final Report											★			
Preparation & Submission of Dissertation (soft bound)								■	■	■	■	★		
Submission of Technical Paper												★		
Viva													★	
Preparation & Submission of Project Dissertation (hard bound)													■	★

★ Milestone

■ Process

REFERENCES

[1] C.P. Loizou and C.S. Pattichis "Introduction to Ultrasound Imaging and Speckle Noise," in *Despeckle Filtering Algorithms and Software for Ultrasound Imaging*, Morgan & Claypool Publishers, 2008, pp. 3-23.

[2] I. Elamvazuthi M.L. Muhd Zain and K.M. Begam, "Despeckling of ultrasound images of bone fracture using multiple filtering algorithms" *SciVerse ScienceDirect Mathematical and Computer Modelling*, vol. 57, pp. 152-168, 2013.

[3] E. Nadernejad, "Despeckle filtering in medical ultrasound imaging", *Contemp. Eng.Sci*., vol. 2, no. 1, pp. 17–36, 2009.

[4] S. Sudha, G.R. Suresh, R. Sukanesh, "Speckle noise reduction in ultrasound images by wavelet thresholding based on weighted variance", *Int. J. Comput.Theory Eng.*, vol. 1, no. 1, pp. 7–12, 2009.

[5] J.S. Lee, "Refined filtering of image noise using local statistics," *Computer Vision, Graphics and Image Processing*, vol.15, pp. 380-389, 1981.

[6] D. T. Kuan, A.A. Sawchuck, T.C. Strand, and P. Chavel, "Adaptive restoration of images with speckle," *IEEE Trans. Acoustics, Speech and Signal Processing*, vol. 1, no. 3, pp. 373-383, 1987.

[7] A. Loper, "Adaptive speckle filters and scene heterogeneity," *IEEE Trans.Geoscience and Remote Sensing*, vol. 28, no.6, pp. 992-1000, Nov.1990.

[8] S. Solbo and T. Eltoft, "Homomorphic wavelet based-statistical despeckling of SAR images," *IEEE Trans. Geosci. Remote Sens.*, vol. 42, no. 4, pp. 711-721, 2004.

[9] R. Perona and J. Malik, "Scale-space and edge detection using anisotropic diffusion," IEEE Trans. Pattern Anal. Mach. Intell., vol.12, no.7, pp. 629-639, July 1990.

[10] Y. Yongjian and S.T. Acton, "Speckle reducing anisotropic diffusion." *IEEE Trans. Image Process*, vol. 11, no. 11, pp. 1260-1270, Nov. 2002.

[11] L. Zhang, P. Bao, and X. Wu, "Multiscale LMMSE-Based Image Denoising With Optimal Wavelet Selection" *IEEE Trans. Circuits and Systems For Video Technology*, vol. 15, No. 4, pp. 469-481, April 2005.

[12] A. Buades, B. Coll, and J. M. Morel, "Image Denoising By Non-Local Averaging" in Computer Vision and Pattern Recognition, 2005. CVPR 2005. *IEEE Computer Society Conference*, vol. 2, pp. 60-65, 2005.

[13] T. Joel and R. Sivakumar, "Despeckling of Ultrasound Medical Images: A Survey" *in Journal of Image and Graphics*, vol. 1, no. 3, pp. 161-164, Sept. 2013.

[14] R. Sivakumar, M.K. Gayathri and D. Nedumaran, "Speckle Filtering Of Ultrasound B-Scan Images-A Comparative Study Between Spatial And Diffusion Filters", *IEEE Conference on Open Systems (ICOS 2010)*, December 2010.

[15] P.C. Tay et al., "Ultrasound Despeckling for Contrast Enhancement" *IEEE Trans. Image Processing*, vol. 19, no. 7, pp. 1847-1860, July 2010.

[16] S. Finn, M. Glavin and E. Jones, "Echocardiographic Speckle Reduction Comparison." *IEEE Trans. Ultrasonics, Ferroelectrics and Frequency Control*, vol.58, no. 1, pp. 82-101, Jan. 2011.

[17] W. Chen, M. Ding, Y. Miao, and L. Luo, "Ultrasound image denoising with multi- shape patches aggregation based non-local means" *International Conference on Intelligent Computation and Bio-Medical Instrumentation*, pp. 35-38, 2011.

[18] V. Karnati, M. Uliyar, and S. Dey "Fast non-local algorithm for image denoising," in *Proc. of IEEE ICIP*, Cairo, Egypt, 2009.

[19] L. Zhang and P. Bao,"Edge detection by scale multiplication in wavelet domain," *Pattern Recognit. Lett*., vol. 23, pp. 1771–1784, 2002.

[20] S. G. Chang, B. Yu, and M. Vetterli,"Adaptive wavelet thresholding for image denoising and compression," *IEEE Trans. Image Process.*, vol. 9,no.9, pp. 1532–1546, Sep. 2000.

[21] G. Fan and X. G. Xia,"Improved hidden Markov models in the wavelet-domain,"*IEEE Trans. Signal Process.*, vol. 49, no. 1, pp. 115–120, Jan 2001.

[22] Y. Cui, T. Zhang, S. Xu and W. Yu, "Image Despeckling Based on LMMSE Wavelet Shrinkage", *Dalian Nationalities University Electrical Review,* pp. 269-272, 2012.

[23] N. Yahya, Nidal S. Kamel, Aamir S. Malik, Subspace-based Technique for Speckle Noise Reduction in SAR Images, IEEE Transactions on Geoscience and Remote Sensing., vol. xx, no. xx, pp.1–15, 2014.

[24] S. Wu, Q. Zhu, and Y. Xie, "Evaluation of various speckle reduction filters on medical Ultrasound images" 35th Annual International Conference of the IEEE EMBS, pp. 1148-1150, July 2013.

[25] R. Ma, X. Zhang and M. Ding, "Quantitative Study on Despeckle Methods of Medical Ultrasound Images" *International Conference on Intelligent Computation and Bio-Medical Instrumentation*, pp. 120-123, 2011.

APPENDICES

MATLAB Code:

a) Denoising and PSNR evaluation code mainly used for Simulated Speckled Test Images Denoising

```
clc;clear all; close all
x     = double(imread('boat (128x128).jpg'));
x     = x(:,:,1);
[K,L] = size(x);

%%%%%%%%%%%%%%%---- Adding speckle noise ----%%%%%%%%%%%%%
v    = 0.1;
n1   = specklegengam(K,L,1/v);
n2   = specklegengam(K,L,1/v);%n10   = specklegengam(K,L,1/v);
n3   = specklegengam(K,L,1/v);%n11   = specklegengam(K,L,1/v);
n4   = specklegengam(K,L,1/v);%n12   = specklegengam(K,L,1/v);
n    =(n1+n2+n3+n4)/4;
y    = x.*n;
figure;imshow(y,[]); title('noisy')
ly   =relog(y);
ly   =log10(ly);
pxy = PSNR(x,y);

%%%%%%%%%%%%%%%---- Lee filter ----%%%%%%%%%%%%%
le = Lee(y);
lec =le(5:100,5:100);
xc  =x(5:100,5:100);
pxle = PSNR(xc,lec)

%%%%%%%%%%%%%%---- Wavelet Zhang filter ----%%%%%%%%%%%%%
wlt = zhang(ly,0.1);
wz  = 10.^wlt;
pxwz = PSNR(x,wz)

%%%%%%%%%%%%%%%---- NLM ----%%%%%%%%%%%%%
sigma=30;
nl = NLmeansfilter(y,5,2,sigma);
pxnl = PSNR(x,nl)

%%%%%%%%%%%%%%%---- SRAD ----%%%%%%%%%%%%%
srad=DsFsrad(y,500,0.025,[3 3 3 3]);
pxsrad = PSNRSRAD(x,srad);

tpsnr = [pxy pxsrad pxle pxwz pxnl]
close all
figure;imshow(x,[]); title('ori')
figure;imshow(y,[]); title('noisy')
figure;imshow(le,[]);title('Lee')
figure;imshow(wz,[]);title('Wavelet')
figure; imshow(nl,[]);title('NLM')
figure;imshow(srad,[]); title('srad')
```

b) Excerpt of USDSAI evaluation code for simulated speckled noise images

```
%%%%%%%%%%%%----USDSAI----%%%%%%%%%%%%
xa = 15:37; ya = 13:26;
xb = 11:33; yb = 106:117;
xc = 57:76; yc = 26:37;
oria  = x(ya,xa);na = y(ya,xa);la  = le(ya,xa);nla = nl(ya,xa);wa  =
wz(ya,xa);sa  = srad(ya,xa);
orib  = x(yb,xb);nb = y(yb,xb);lb  = le(yb,xb);nlb = nl(yb,xb);wb  =
wz(yb,xb);sb  = srad(yb,xb);
oric  = x(yc,xc);nc = y(yc,xc);lc  = le(yc,xc);nlc = nl(yc,xc);wc  =
wz(yc,xc);sc  = srad(yc,xc);
qx  = Qcyst(oria,orib,oric);
qy  = Qcyst(na,nb,nc);
qnl = Qcyst(nla,nlb,nlc);
qad = Qcyst(sa,sb,sc);
qw  = Qcyst(wa,wb,wc);
ql  = Qcyst(la,lb,lc);

usdsai = [qx qy ql qw qnl qad]/qx
```

c) Excerpt of normalized variance and mean preservation evaluation code

```
function out = NormVar(I)
% [nRows, nCols] = size(I);
iMean = mean(I(:));
% imgVar = (double(I(:)) - imgMean)' * (double(I(:)) - imgMean) /
(nRows * nCols);
iVar = var(I(:));
imgVar = iVar/iMean^2;
out = [imgVar;iMean];
```